DINAME 2017 - Proceedings of the XVII International Symposium on Dynamic Problems of Mechanics
A. T. Fleury, D. A. Rade, P. R. G. Kurka (Editors), ABCM, São Sebastião, SP, Brazil, March 5-10, 2017

THE MECHANICAL BEHAVIOUR OF VISCOELASTIC MATERIALS IN THE FREQUENCY DOMAIN

Isadora R. Henriques[1], **Lavinia A. Borges**[1], **Daniel A. Castello**[1]

[1] Mechanical Engineering Department
Universidade Federal do Rio de Janeiro
21.941-972 - Rio de Janeiro - RJ, Brazil, P.O. Box 68.503
ir.henriques@mecanica.coppe.ufrj.br, lavinia@mecanica.ufrj.br, castello@mecanica.ufrj.br

Abstract: In the last few decades, a growing need for new materials for dedicated and complex applications led to the development of approaches to model their physical behaviour. Among these one may cite viscoelastic materials, shape memory alloys and Functionally Graded Materials. As for viscoelastic materials, great efforts have been done to understand and characterize the one-dimensional behavior throughout moduli such as complex modulus, ignoring the role of the viscoelastic Poisson's ratio. There are just a few studies carried out for this property as well as no consolidated experiments to estimate it despite its importance in the complete characterization of viscoelastic materials. The purpose of this work is to determine the viscoelastic Poisson's ratio in the frequeny domain, $\nu^*(\omega)$, for a viscoelastic material in order to characterize its three-dimensional behavior. To do so, the work is based on the elastic-viscoelastic correspondence principle (EVCP) and the time-temperature superposition principle (TTSP). Measurements of the complex shear modulus, $G^*(\omega)$, and the complex modulus, $E^*(\omega)$, were performed using a dynamic mechanical analyzer (DMA). To consider eventual uncertainties, the tests were carried out at three test-specimens.

Keywords: 3D Viscoelasticity, Characterization, Poisson's Ratio, Complex Modulus, Dynamic Mechanical Analysis.

INTRODUCTION

Viscoelastic materials are used in many applications such as structural components to control vibrations (Hernández et al., 2016) (Borges *et al.*, 2015) (Rouleau *et al.*, 2015), tooth reconstruction (Dauvillier *et al.*, 2000), adhesives (Estrada-Royval and Díaz-Díaz, 2015), among others. As the fields of applications have been continuously grown, several studies aim at characterizing and predicting the mechanical behaviour of these materials focusing on the complex moduli such as complex Young's modulus. Nevertheless, the study of *Poison's ratio (PR)* for this type of materials remains ambiguous and incomplete, lacking experimental procedures to its determination. On many studies, this ratio is considered to be constant even though the thermo-temporal dependency of PR is supported by experimental evidence as early as 1987 (Hilton, 2001).

The Poisson's ratio (PR) of a viscoelatic material is a function of time (or frequency) that does not present a well established definition (Hilton, 2001). For its frequency dependence, it can also be seen as a complex number known as complex Poisson's ratio with its real part known as dynamic Poisson's ratio and its imaginary part known as loss component. The imaginary part is related to a phase lag between the lateral and axial strains. Both parts of this ratio are frequency and thermal dependent, presenting a much more complex behaviour and difficulty on its experimental characterization (Pritz, 2007). Additionaly, it can be determined once one obtains the complex modulus and complex shear modulus (Tschoegl *et al.*, 2002).

Many techniques to measure viscoelastic properties as a function of temperature and frequency are available in the literature and are reviewed by (Lakes, 2004). Among them, one of the most common methods used is the dynamic mechanical analysis (DMA) in which a sinusoidal excitation is applied to a test-specimen and its response is then measured at different frequencies and temperatures. This technique allows us to have more information about the material than the techniques involving static tests; moreover, it also provides different tests at the same conditions.

This work aims to determine the complex Poisson's ratio, $\nu^*(\omega)$, through experiments carried out using a Dynamic Mechanical Analyzer (DMA) in order to characterize the three-dimensional behavior of viscoelastic materials. The complex modulus, $E^*(\omega)$, and the complex shear modulus, $G^*(\omega)$, were measured in two different operational modes: single cantilever bending and simple shear modes, respectively. The elastic-viscoelastic correspondence principle (EVCP) (Lee, 1961) was employed to obtain the viscoelastic relation between these properties. The thermorheologically simple behavior of the material was also verified by the Cole-Cole Diagram and the Black Space and consequently, the time-temperature superposition principle (TTSP) (Dealy and Plazek, 2009) was applied to build the master curves.

FUNDAMENTALS

Complex Poisson's Ratio, $\nu^*(\omega)$

In the theory of linear viscoelasticity, the Poisson's ratio does not have a unique definition. It is rather defined in several ways ranging from six different categories sorted by their physical meaning as stated by (Hilton, 2011). However, all the definitions present an important similarity: the Poisson's ratio is not a constant value, presenting a time- or frequency-dependent function as well as other viscoelastic material properties.

According to (Tschoegl *et al.*, 2002), the frequency-dependent (or complex) Poisson's ratio corresponds to the lateral contraction ratio measured in an infinitesimally small uniaxial deformation of a viscoelastic material in response to a steady-state sinusoidally oscillating strain. Mathematically, it may be expressed as

$$\nu_{j1}^*(\omega) = -\frac{\varepsilon_{jj}^*(\omega)}{\varepsilon_{11}^0}, \, j \neq 1 \tag{1}$$

where ε_{11}^0 is the amplitude of the sinusoidal steady-state strain, $\varepsilon_{jj}^*(\omega)$ is the complex sinusoidal steady-state lateral contraction and ω, the frequency in radians per second.

Being a complex property, it can be decomposed in its real and imaginary parts. The former is associated with the elastic response (stored energy), whereas the latter is associated with the viscous response (energy dissipation). Thus, in Cartesian coordinates,

$$\nu^*(\omega) = \nu'(\omega) - j\nu''(\omega) = \nu'(\omega)[1 - j\eta_\nu(\omega)], \tag{2}$$

where $\nu'(\omega)$ is the dynamic Poisson's ratio and $\nu''(\omega)$ is the loss component and $\eta_\nu(\omega)$ is the Poisson's loss factor defined as (Pritz, 2007)

$$\eta_\nu(\omega) = \frac{\nu''(\omega)}{\nu'(\omega)}. \tag{3}$$

In case of perfect elasticity, the loss component is zero and, consequently, Poisson's loss factor is also zero. In addition, the negative sign in Eq. (2) is related to the compliance nature of the viscoelastic PR (Tschoegl *et al.*, 2002).

The absolute value of complex PR can be obtained through

$$|\nu^*(\omega)| = \sqrt{\nu'(\omega)^2 + \nu''(\omega)^2} \tag{4}$$

Furthermore, the complex PR can be determined indirectly through any two other viscoelastic function using the elastic-viscoelastic correspondence principle (EVCP). The elastic interrelationship between the Young's modulus E, the shear modulus G, and the Poisson's ratio ν is given as follows:

$$\nu = \frac{E}{2G} - 1. \tag{5}$$

Thus, the viscoelastic interrelationship in frequency domain due to EVCP is

$$\nu^*(\omega) = \frac{E^*(\omega)}{2G^*(\omega)} - 1, \tag{6}$$

where $E^*(\omega)$ is the complex modulus and $G^*(\omega)$, the complex shear modulus.

The real and imaginary parts of complex PR can be written in terms of the real and imaginary parts of complex modulus ($E'(\omega)$, $E''(\omega)$) and complex shear modulus ($G'(\omega)$, $G''(\omega)$) as follows

$$\nu'(\omega) = \frac{1}{2}\frac{E'(\omega)G'(\omega) + E"(\omega)G"(\omega)}{[G'(\omega)]^2 + [G"(\omega)]^2} - 1 \tag{7}$$

and

$$\nu''(\omega) = \frac{1}{2}\frac{E'(\omega)G"(\omega) - E"(\omega)G'(\omega)}{[G'(\omega)]^2 + [G"(\omega)]^2}. \tag{8}$$

EXPERIMENTAL RESULTS

Materials

The family of polymers analyzed in this work was produced from a pure epoxy prepolymer to which none or a certain amount of flexibilizer was added. The epoxy resin was Es260 br, a cold-setting one. *Aradur*^{TM} E35, a cycloaliphatic amine based curing agent with low viscosity, was used as hardener for the curing process. Finally, the flexibilizer used was DY 3601. All reagents were purchased from Advanced Vacuum Materials (São Paulo, Brazil).

Firstly, a mixture of epoxy resin and curing agent in a proportion of 45 phr were poured in a becker and were gently mixed using a glass tube. Afterwards, half of the mixture was carefully transferred to a second becker and both beckers were weighted to ensure their equal content. Then, the flexibilizer was added to the first becker in a proportion corresponding to 10% by weight of the mixture and this new epoxy system was mixed again to homogenize it. Finally, both beckers were put on an ultrasonic bath for 30 minutes to avoid the presence of air bubbles. After the bath, the mixtures were poured into the cavities of silicone rubber molds with appropriate dimensions for the tests. The curing process was performed at room temperature for 24h, followed by a post-curing cycle at $60°C$ for 6h in an oven. To avoid residual stresses, the test-specimens were then slowly cooled to room temperature inside the oven. Three test-specimens were manufactured for each test and for each material within the same batch in order to ensure material repeatability.

Tests by DMA

Dynamic tests were carried out with a DMA Q800 dynamic mechanical analyzer (produced by TA Instrument Corporation) to investigate the complex modulus $E^*(\omega)$ and the complex shear modulus $G^*(\omega)$. For that purpose, the testing configuration was set in two different operational modes, respectively: single cantilever bending mode and simple shear mode. The former consists of a test-specimen anchored on one end by a stationary clamp and by a moveable clamp on the other which applies a controlled force. The test-specimen's dimensions are 25.0 mm x 7.0 mm x 2.0 mm. The latter consists of two equal-size test-specimens sheared between a fixed and a moveable plate. In this situation, the test-specimen's dimensions are 10.0 mm x 10.0 mm x 2.5 mm.

For both operational modes, frequency sweeps from 1 to 100Hz, measuring 10 points per decade in logarithm scale, were carried out at fourteen temperatures from 60 to $90°C$. Isotherms were maintained for 5 minutes every $5°C$ and the heating rate was $2°C/min$.

RESULTS AND DISCUSSIONS

Each test was performed on three test-specimens of each material to reduce experimental errors. The results shown next are an average of each material.

Complex Modulus, $E^*(\omega)$

Figure 1 shows the real part of complex modulus, also known as storage modulus and denoted by $E'(\omega)$, as a function of frequency for both materials. It decreased with the increase in temperature and increased with the increase in frequency, especially at high temperatures and for epoxy with flexibilizer. For all temperature range, pure epoxy presents a higher modulus.

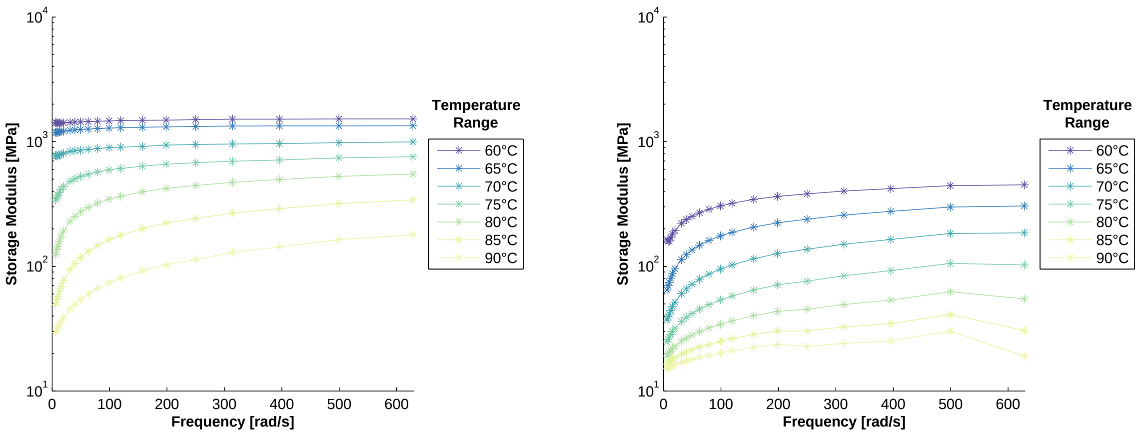

(a) Pure Epoxy

(b) Epoxy with Flexibilizer

Figure 1: Storage Modulus $(E'(\omega))$ *versus* Frequency (ω).

The imaginary part of complex modulus, known as loss modulus and denoted by $E''(\omega)$, is then represented in Fig. 2. For pure epoxy, below $80°C$, it increased with the in increase in temperature and did not vary with the frequency. From $80°C$, it decreased with the increased in temperature and increased with the increase in frequecy. For epoxy with flexibilizer, on the other hand, it presented a similar behavior as its real part.

In order to apply the time-temperature superposition principle (TTSP) (Dealy and Plazek, 2009) to characterize the materials on a broader frequency range, the thermo-rheolocally simple behavior of these materials was verified through the Cole-Cole Diagram (Dae Han and Kim, 1993) (Fig. 3) and the Black Space (Van Gurp and Palmen, 1998) (Fig. 4). In both diagrams, most points lied close to one single curve. Points that deviate from the curves are related to measurements at high frequencies and they may be related to resonance phenomena in the DMA (Placet and Foltête, 2010). Additionally, both diagrams show a slight temperature dependence of complex modulus of both materials, indicating a need for vertical

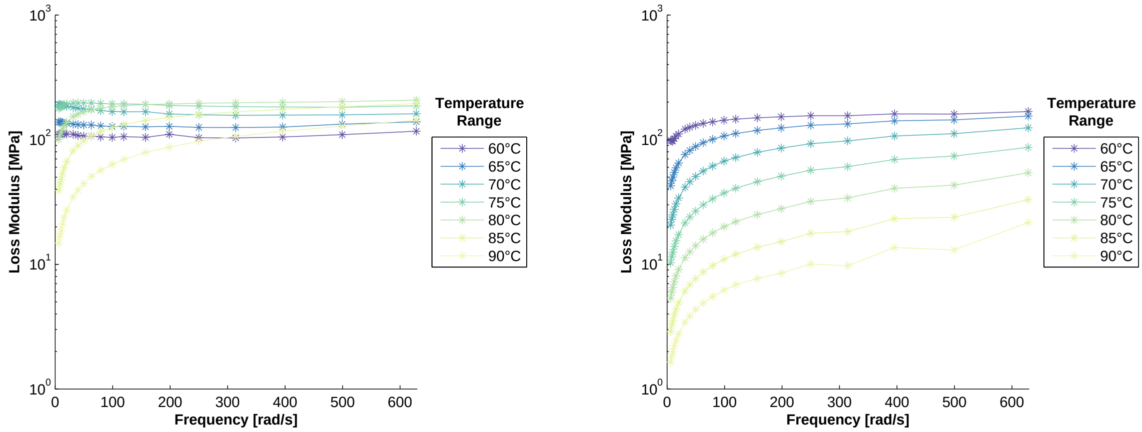

(a) Pure Epoxy (b) Epoxy with Flexibilizer

Figure 2: Loss Modulus $(E''(\omega))$ *versus* Frequency (ω).

shifting (Rouleau *et al.*, 2013).

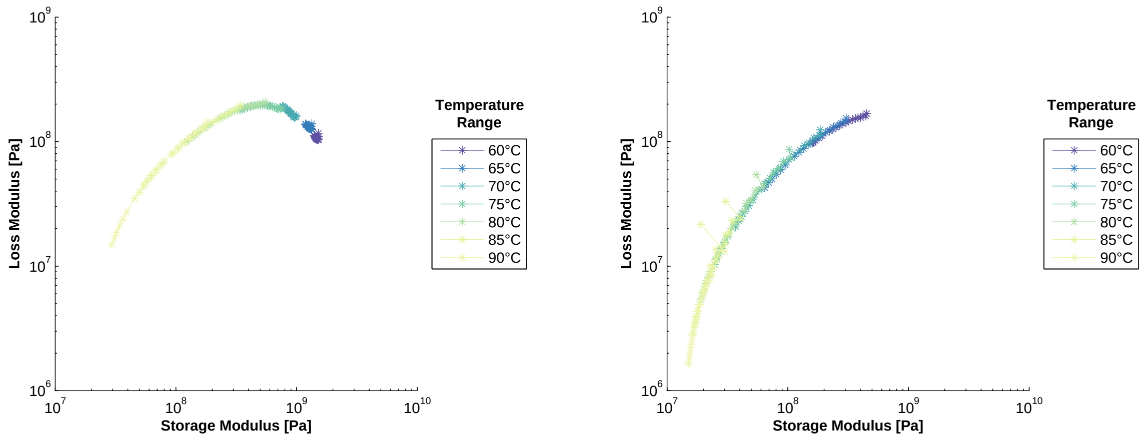

(a) Pure Epoxy (b) Epoxy with Flexibilizer

Figure 3: Cole-Cole Diagrams: $E''(\omega)$ *versus* $E'(\omega)$.

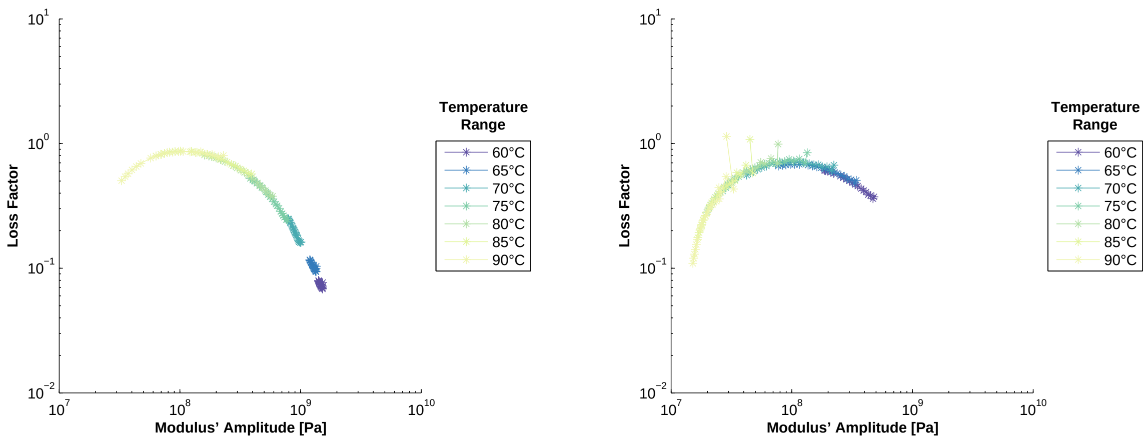

(a) Pure Epoxy (b) Epoxy with Flexibilizer

Figure 4: Black Diagrams: $E''(\omega)/E'(\omega)$ *versus* $|E^*(\omega)|$.

The thermal shift factor (a_T), also known as horizontal shift coefficient (Dealy and Plazek, 2009), is required for TTSP and was then estimated. They were computed for all three test-specimens as a function of the relative temperature and were fitted by the Williams-Landel-Ferry (WLF) equation (Williams *et al.*, 1955):

$$\log a_T = -\frac{C_1(T - T_0)}{C_2 + (T - T_0)}, \tag{9}$$

with T_0 as the reference temperature in Kelvin, T as the temperature in Kelvin and C_1 and C_2 as empirical constants that depend on the material and the reference temperature.

The reference temperature was $348K$ and the parameters $C_1 = 19.07$ and $C_2 = 43.17K$ were estimated for pure epoxy system, while $C_1 = 15.28$ and $C_2 = 68.41K$ for epoxy with flexibilizer. From Fig. 5, it can be observed that the thermal shift factor a_T presents high levels of correlation with measured data.

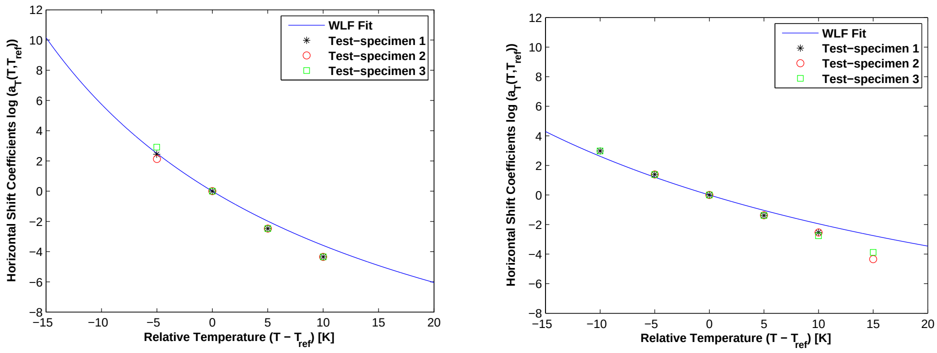

(a) Pure Epoxy: $C_1 = 19.07$ and $C_2 = 43.17K$ (b) Epoxy with Flexibilizer: $C_1 = 15.28$ and $C_2 = 68.41K$

Figure 5: Thermal shift factors for WLF Equation from $E^*(\omega)$ - $T_{ref} = 348K$.

Finally, the master curves built by using the method described in (Rouleau *et al.*, 2013) are presented in Fig. 6 and Fig. 7. These curves are not so continuous due to the lack of the vertical shift coefficients, which were not applied in this work.

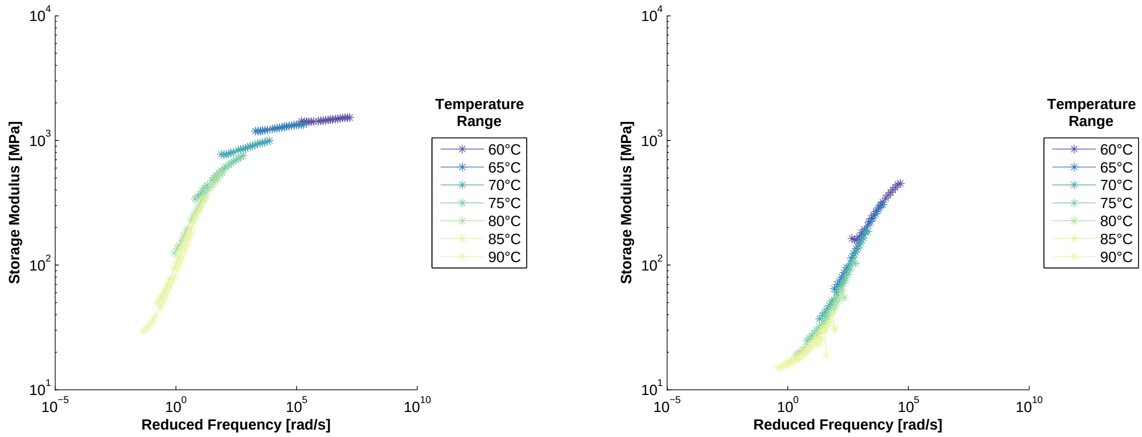

(a) Pure Epoxy (b) Epoxy with Flexibilizer

Figure 6: Master Curves for Storage Modulus $E'(\omega)$.

Complex Shear Modulus, $G^*(\omega)$

The real part of complex shear modulus, known as shear storage modulus and denoted by $G'(\omega)$, is shown in Fig. 8. The imaginary part, known as shear loss modulus and denoted by $G''(\omega)$, is depicted in Fig. 9. The moduli behavior in respect to changes in temperatures and frequencies presented the same pattern of complex modulus.

The assumption of thermo-rheologically simple behavior of these materials was also verified using the results of complex shear modulus. Figure 10 shows the Cole-Cole Diagram and Fig. 11, the Black Space. Again, most points coincided along one single continuous curve and a slight temperature dependence of the material's property can be noted in both diagrams (Rouleau *et al.*, 2013).

In order to validate the model built for the thermal shift factor $a_T(C_1, C_2)$ using the complex modulus, a new model for a_T was then built with the complex shear modulus data. Figure 12 presents the measured data and the model built with the estimated parameters. Figures 5 and 12 show that the models are highly correlated.

The master curves were obtained again using the method described in (Rouleau *et al.*, 2013) at a reference temperature

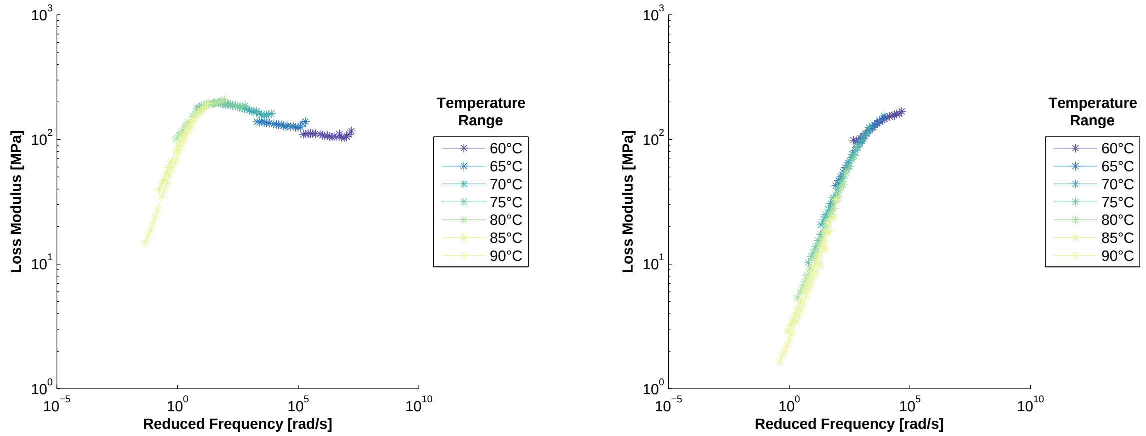

(a) Pure Epoxy (b) Epoxy with Flexibilizer

Figure 7: Master Curves for Loss Modulus $E''(\omega)$.

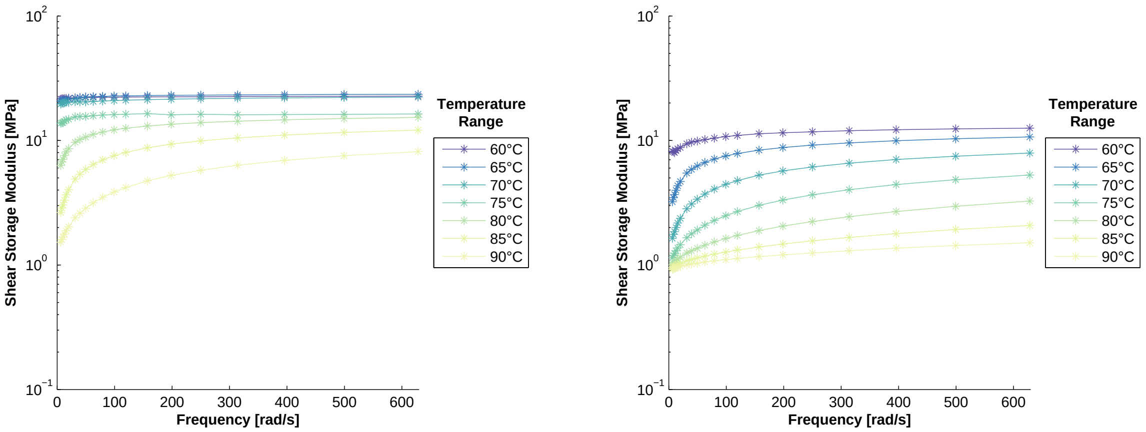

(a) Pure Epoxy (b) Epoxy with Flexibilizer

Figure 8: Shear Storage Modulus $(G'(\omega))$ *versus* Frequency (ω).

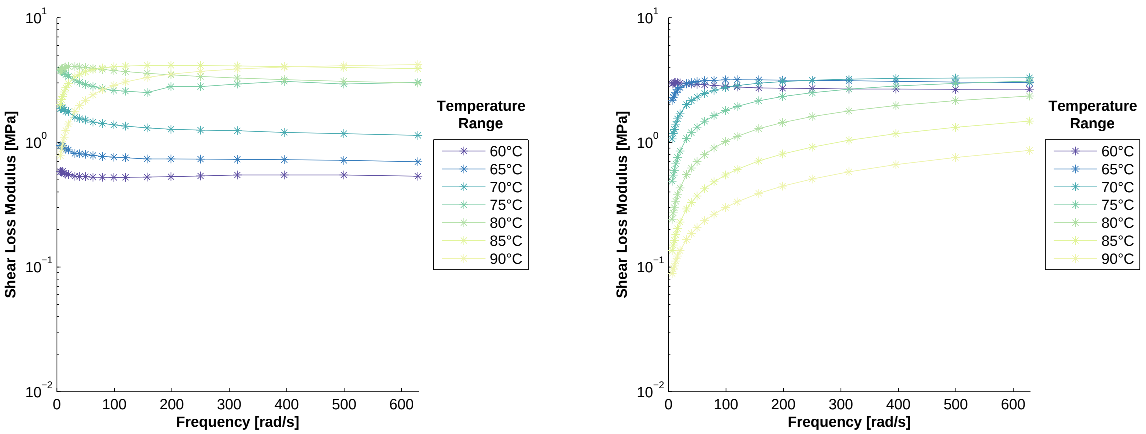

(a) Pure Epoxy (b) Epoxy with Flexibilizer

Figure 9: Shear Loss Modulus $(G''(\omega))$ *versus* Frequency (ω).

of $348K$. Figures 6 and 7 show, respectively, the master curves of shear storage modulus and shear loss modulus. In pure epoxy, they are not so continuous due to the lack of the vertical shift coefficients, which were not applied in this work.

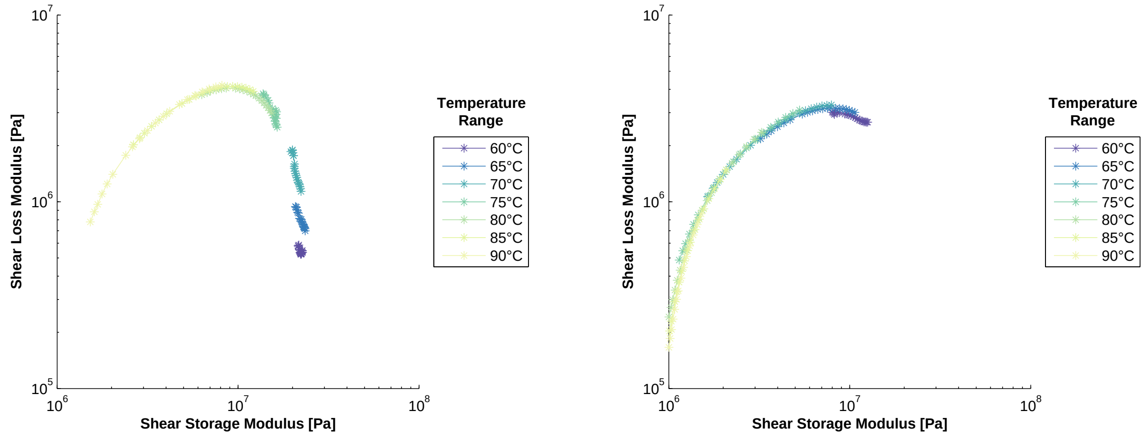

(a) Pure Epoxy (b) Epoxy with Flexibilizer

Figure 10: Cole-Cole Diagrams: $G''(\omega)$ *versus* $G'(\omega)$.

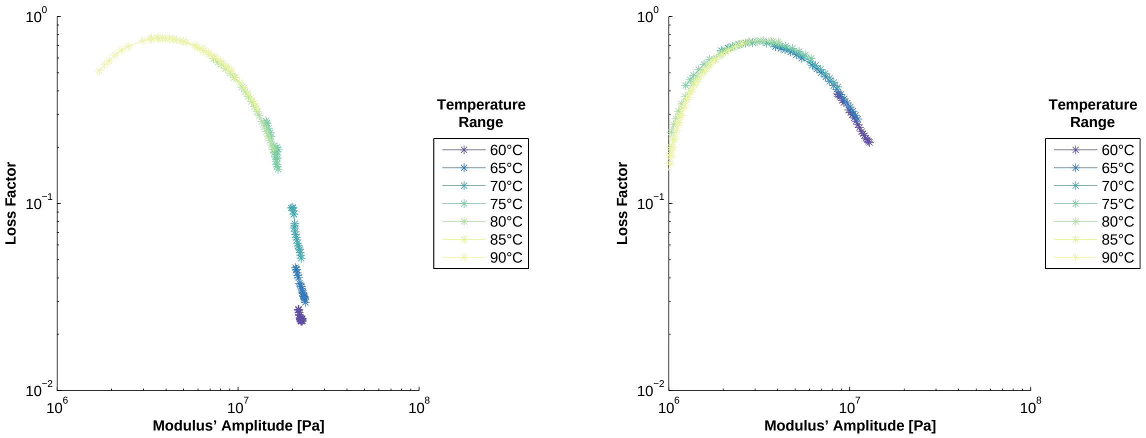

(a) Pure Epoxy (b) Epoxy with Flexibilizer

Figure 11: Black Diagrams: $G''(\omega)/G'(\omega)$ *versus* $|G^*(\omega)|$.

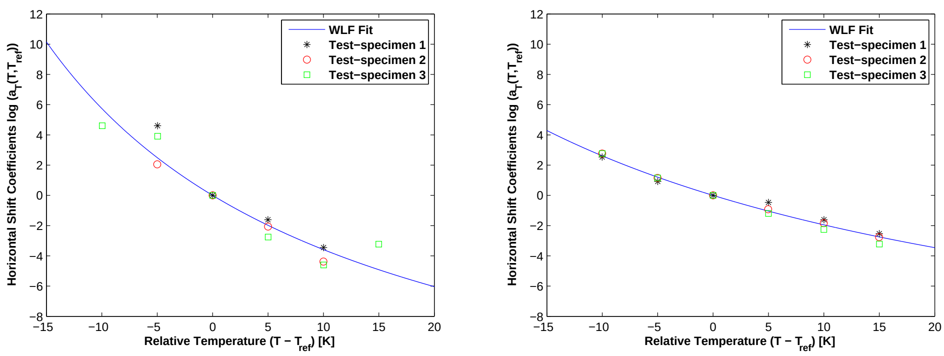

(a) Pure Epoxy: $C_1 = 19.07$ and $C_2 = 43.17K$ (b) Epoxy with Flexibilizer: $C_1 = 15.28$ and $C_2 = 68.41K$

Figure 12: Thermal shift factors for WLF Equation from $G^*(\omega)$ - $T_{ref} = 348K$.

Complex Poisson's Ratio, $\nu^*(\omega)$

The dynamic Poisson's ratio and the loss component were thus determined using the real and imaginay components of complex modulus and complex shear modulus through Eq. (7) and Eq. (8). However, the results were not consistent with the limits of 0.5 and -1 (**?**). A further look on the experimental apparatus revealed a sistematic error due to a scale factor also reported by (Kumar, 2016) (Swaminathan and Shivakumar, 2008) (Deng *et al.*, 2007). To solve this issue, a correction was applied. The results of complex shear modulus were compared to the ones reported by (Rao *et al.*, 2014), generating a scale factor. It is worth noting that the shift factors for temperatures close to glass transition was quite difficult

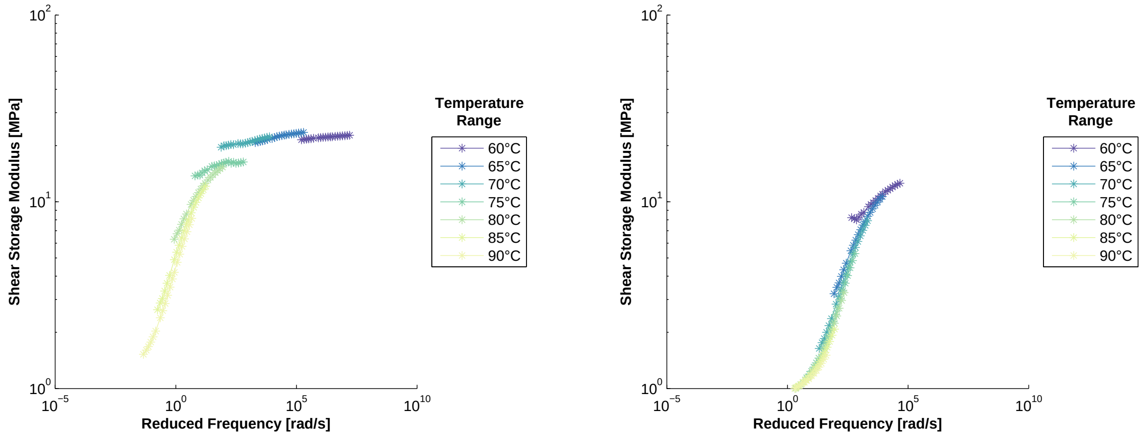

(a) Pure Epoxy (b) Epoxy with Flexibilizer

Figure 13: Master Curves for Shear Storage Modulus $G'(\omega)$.

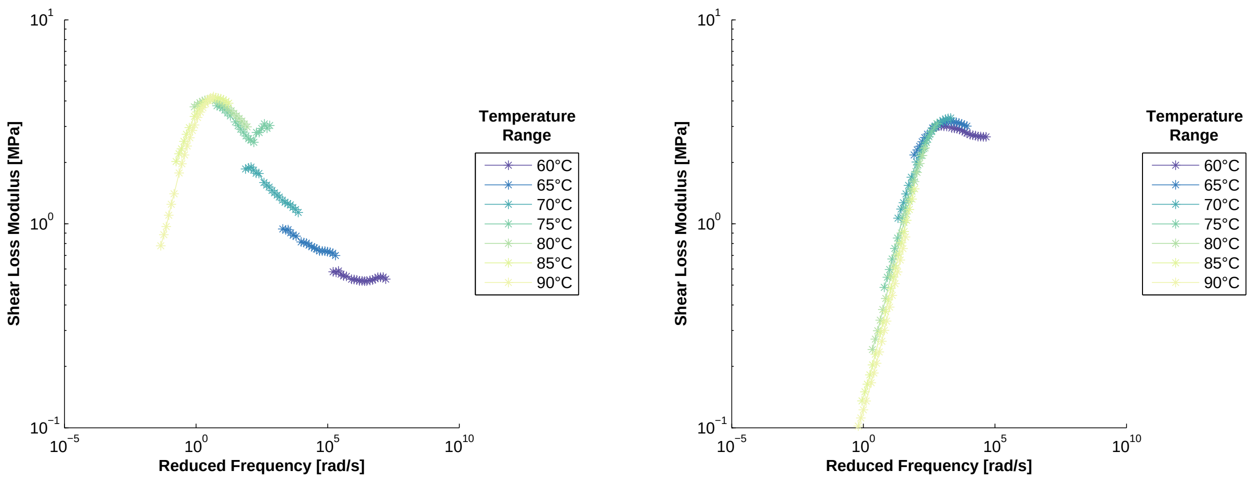

(a) Pure Epoxy (b) Epoxy with Flexibilizer

Figure 14: Master Curves for Shear Loss Modulus $G''(\omega)$.

to identify due to great variations of the moduli in this range.

Figures 15, 16 and 17 show, respectively, the results obtained for $\nu'(\omega)$, $\nu''(\omega)$ and $|\nu^*(\omega)|$ for each material. For pure epoxy, below $75°C$, the dynamic Poisson's ratio and the loss component are almost constant over the frequency range. However, above $75°C$, the dynamic Poisson's ratio increases with the frequency whereas the loss component decreases. For epoxy with flexibilizer, on the other hand, the dynamic Poisson's ratio increases with the frequency, whereas the loss component decreases.

CONCLUSIONS

This work proposes an approach to estimate the complex Poisson's ratio through an indirect method. The complex modulus and the complex shear modulus were first determined by performing two different tests using a dynamic mechanical analyzer. The influence of frequency and temperature was observed in these viscoelastic properties. Throughout the Cole-Cole diagram and Black Space, the thermo-rheologically simple behavior was identified in all materials. As the estimations for complex Poisson's ratio were meaningless from the physical point of view, a scale factor was used to calculate the material properties and produce results within acceptable values. A key point to be emphasized is that investigations in the literature have indicated that there is a great discrepancy in scale with the data provided by the DMA as reported in (Kumar, 2016) (Swaminathan and Shivakumar, 2008) (Deng *et al.*, 2007) and in most cases, DMA data is used for examining material properties for quality control, research and development, and also for the establishment of optimum processing conditions. Although DMA did not characterize quantitatively this property in a high stiff viscoelastic material, a natural progression is to verify if the methodology applied can be used on low stiff ones.

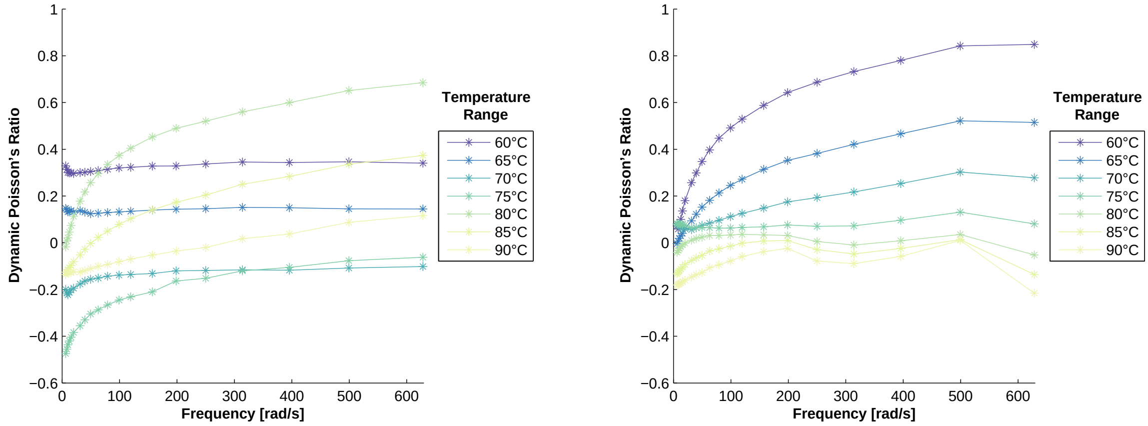

(a) Pure Epoxy (b) Epoxy with Flexibilizer

Figure 15: Dynamic Poisson's Ratio $(\nu'(\omega))$ *versus* Frequency (ω).

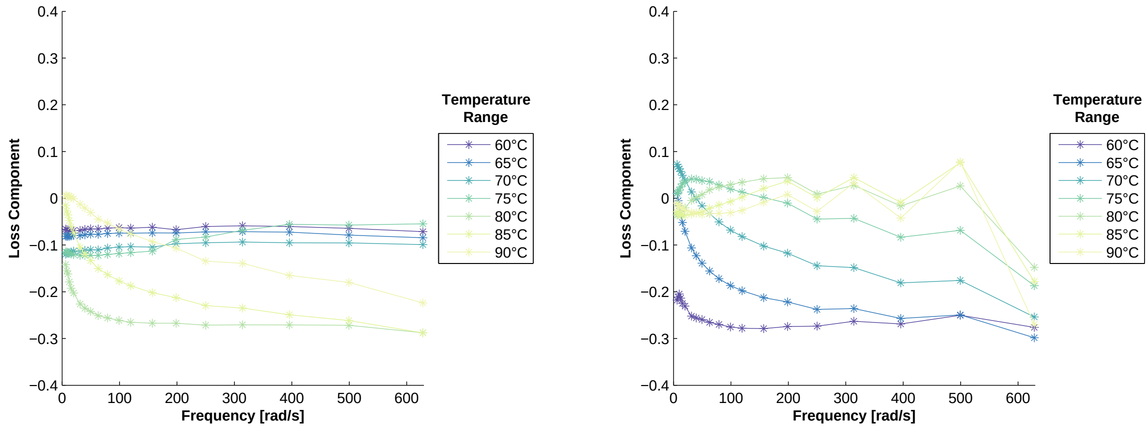

(a) Pure Epoxy (b) Epoxy with Flexibilizer

Figure 16: Loss Component $(\nu''(\omega))$ *versus* Frequency (ω).

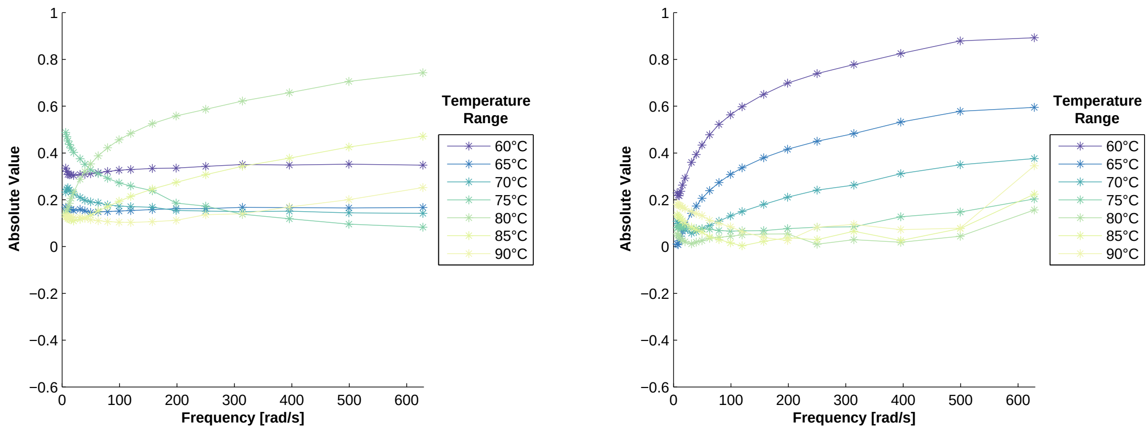

(a) Pure Epoxy (b) Epoxy with Flexibilizer

Figure 17: Absolute Value $(|\nu^*(\omega)|)$ *versus* Frequency (ω).

ACKNOWLEDGMENTS

The authors would like to express their gratitude to the National Council for Scientific and Technological Development (CNPq) for its financial support under grant number 483391/2013, to Coordenação de Aperfeiçoamento de Pessoal de Nível Superior (CAPES) for its financial support under grant number AUXPE n.1197/2014, to the National Foundation of

Studies and Projects (FINEP) for its financial support [grant number 01.12.0226.00.]

REFERENCES

Borges, F.C.L., Castello, D.A., Magluta, C., Rochinha, F.A. and Roitman, N., 2015, "An experimental assessment of internal variables constitutive models for viscoelastic materials", Mechanical Systems and Signal Processing, 50-51(1), pp. 27–40.

Dae Han, C., and Kim, J.K., 1993, "On the use of time-temperature superposition in multicomponent/multiphase polymer systems", Polymer, 34(12), pp. 2533–2539.

Dauvillier, B.S., Feilzer, A.J., De Gee, A.J., and Davidson, C.L., 2000, "Visco-elastic parameters of dental restorative materials during setting", Journal of dental research, 79(3), pp. 818–823.

Dealy, J., and Plazek, D., 2009, "Time-Temperature Superposition - A Users Guide", Rheology Bulletin, 78, pp. 16–31.

Deng, S., Hou, M., and Ye, L., 2007, "Temperature-dependent elastic moduli of epoxies measured by DMA and their correlations to mechanical testing data", Polymer Testing, 26(6), pp. 803–813.

Estrada-Royval, I.-A., and Díaz-Díaz, A., 2015, "Post-curing process and visco-elasto-plastic behavior of two structural adhesives", International Journal of Adhesion and Adhesives, 61(9), pp. 99–111.

Greaves, G.N., Greer, A.L., Lakes, R.S., and Rouxel, T., 2011, "Poisson's ratio and modern materials", Nature Materials, 10(11), pp. 823–837.

Hernández, W.P., Castello, D.A., and Ritto, T.G., 2016, "Uncertainty propagation analysis in laminated structures with viscoelastic core", Computers & Structures, 164(2), pp. 23–37.

Hilton, H., 2011, "Clarifications of Certain Ambiguities and Failings of Poisson's Ratios in Linear Viscoelasticity", Journal of Elasticity, 104(1), pp. 303–318.

Kumar, N.P., 2016, "Viscoelastic Characterization and Effective Damping of a Carbon/Polyurethane Laminate", Master Thesis, Rochester Institute of Technology, New York.

Lakes, R.S., 2004, "Viscoelastic measurement techniques", Review of Science Instrument, 75(4), pp. 797-810.

Lee, E.H., 1961, "Stress analysis for linear viscoelastic materials", Rheologica Acta, 1(4-6), pp. 426–430.

Pandini, S., and Pegoretti, A., 2008, "Time, temperature, and strain effects on viscoelastic Poisson's ratio of epoxy resins", Polymer Engineering and Science, 48(7), pp. 1434–1441.

Placet, V., and Foltête, E., 2010, "Is Dynamic Mechanical Analysis (DMA) a non-resonance technique?", EPJ Web of Conferences, 6, pp. 41004.

Pritz, T., 2007, "The Poisson's loss factor of solid viscoelastic materials", Journal of Sound and Vibration, 306(3), pp. 790–802.

Rao, K.V., Dayananda, G.N., and Ananthapadmanabha, G.S., 2014, "Viscoelastic Characterisation of an Epoxy based Shape Memory Polymer (SMEP)", Indian Journal of Advances in Chemical Science, 2, pp. 64–67.

Rouleau, L., Deu, J.-F., Legay, A., and Le Lay, F., 2013, "Application of Kramers–Kronig relations to time–temperature superposition for viscoelastic materials", Mechanics of Materials, 65(10), pp. 66–75.

Rouleau, L., Pirk, R., Pluymers, B., and Desmet, W., 2015, "Characterization and Modeling of the Viscoelastic Behavior of a Self-Adhesive Rubber Using Dynamic Mechanical Analysis Tests", Journal Aerospace Technology Management, 7(2), pp. 200–208.

Swaminathan, G., and Shivakumar, K., 2008, "A Re-examination of DMA Testing of Polymer Matrix Composites", Journal of Reinforced Plastics and Composites, 28(8), pp. 979–994.

Tschoegl, N.W., 1989, "The Phenomenological Theory of Linear Viscoelastic Behavior", Berlin, Heidelberg: Springer Berlin Heidelberg.

Tschoegl, N.W., Knauss, W.G., and Emri, I., 2002, "Poisson's ratio in linear viscoelasticity – a critical review", Mechanics of Time-Dependent Materials, 6(1), pp. 3–51.

Van Gurp, M., and Palmen, J., 1998, "Time-Temperature Superposition for Polymeric Blends", Rheology Bulletin, 67(1), pp. 5–8.

Williams, M.L., Landel, R.F., and Ferry, J.D., 1955, "The Temperature Dependence of Relaxation Mechanisms in Amorphous Polymers and Other Glass-forming Liquids", Journal of the American Chemical Society, 77(14), pp. 3701–3707.

RESPONSIBILITY NOTICE

The authors are the only responsible for the material included in this paper.